Rheological behavior of high consistency enzymatically fibrillated cellulose suspensions

Jaiswal, Aayush Kumar; Kumar, Vinay; Khakalo, Alexey; Lahtinen, Panu; Solin, Katariina; Pere, Jaakko; Toivakka, Martti

Published in:
Cellulose

DOI:
10.1007/s10570-021-03688-y

Published: 01/03/2021

Document Version
Final published version

Cellulose
https://doi.org/10.1007/s10570-021-03688-y

ORIGINAL RESEARCH

Rheological behavior of high consistency enzymatically fibrillated cellulose suspensions

Aayush Kumar Jaiswal · Vinay Kumar · Alexey Khakalo · Panu Lahtinen · Katariina Solin · Jaakko Pere · Martti Toivakka

Received: 28 September 2020 / Accepted: 7 January 2021

Abstract High-consistency processing of fibrillated cellulose materials is attractive for commercial applications due to potential for lowered production costs, energy savings and easier logistics. The current work investigated structure–property relationships of fibrillated cellulose suspensions produced at 20% consistency using VTT HefCel (High-consistency enzymatic fibrillation of cellulose) technology. Morphological examination of the fibrillated materials revealed that enzymatic action on the cellulose substrates was not a direct function of enzyme dosage but rather was dependent on the raw material composition. Furthermore, shear viscosity of the HefCel suspensions was found to decrease with increasing enzyme dosage while the water retention increased. The shear viscosity followed power law relationship with the power law index varying in the range 0.11–0.73. The shear-thinning behavior decreased with increasing consistency. Moreover, suspension viscosity (μ) was found to be highly dependent on the consistency (c) as $\mu \sim c^m$, with m ranging from 2.75 to 4.31 for different samples. Yield stress (τ_y) of the HefCel suspensions was measured at 7 and 10% consistencies. The performance of the fibrillated cellulose grades in a typical application was demonstrated by casting films, which were characterized for their mechanical properties.

Supplementary Information The online version of this article (https://doi.org/10.1007/s10570-021-03688-y) contains supplementary material, which is available to authorized users.

A. K. Jaiswal (✉) · V. Kumar · A. Khakalo · P. Lahtinen · J. Pere
Biomass Processing and Products, VTT Technical Research Centre of Finland Ltd, Tietotie 4E, 02044 Espoo, Finland
e-mail: aayush.jaiswal@vtt.fi

A. K. Jaiswal · M. Toivakka
Laboratory of Natural Materials Technology, Åbo Akademi University, Porthaninkatu 3, 20500 Turku, Finland

K. Solin
Department of Bioproducts and Biosystems, School of Chemical Engineering, Aalto University, Vuorimiehentie 1, 00076 Espoo, Finland

Published online: 21 January 2021

Graphic abstract

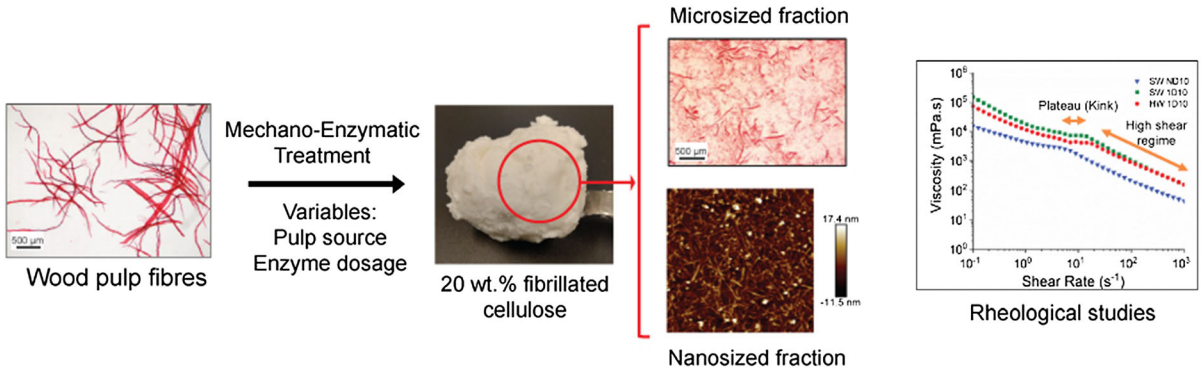

Keywords Cellulose · Enzymatic hydrolysis · Rheology · HefCel · Nanocellulose

Introduction

Lignocellulosic biomass is considered as one of the most promising and sustainable natural resources due to its abundance and renewable nature. Biomass has traditionally been utilized poorly as a fuel but is now rapidly becoming an important raw material for manufacturing biofuels and chemicals, and the need for high-value products obtained from biomass keeps growing (Song et al. 2014).

One among many of such high-value products are cellulose nanomaterials (CNMs), which have been studied for numerous applications such as, in packaging, cell culture, drug delivery, 3D printing, rheology modifications, and electronics (Abitbol et al. 2016; Dufresne 2019; Fang et al. 2019; Plackett 2014). While some applications aim at replacing nonrenewable fossil fuel-based materials in existing products, others target totally novel products. Cellulose nanofibril (CNF) and Cellulose nanocrystal (CNC), the two major grades of nanocellulosic materials, are manufactured by either purely mechanical treatments, or a combination of chemical and mechanical treatment (Abdul Khalil et al. 2014). Chemical pre-treatments reduce energy consumption during the production of CNFs and improve the degree of fibrillation when compared to solely mechanical processes (Malucelli et al. 2019; Siró and Plackett 2010). Another route to obtain CNMs from biomass is biological, via enzymatic pre-treatment of cellulose. Enzymatic pretreatment on pulp fibres has been shown to be an energy efficient method to derive CNMs (Henriksson et al. 2007; Pääkkö et al. 2007).

Enzymatic treatment of cellulose to obtain CNMs has been studied extensively in the past where efforts have been devoted towards identifying enzymes for efficient fibrillation, studying their mechanisms, and developing processes for controlled unraveling of the fibre cell wall to obtain fibrillated cellulosic materials (Karim et al. 2017). Cellulases, especially endoglucanases have been previously used for cellulose fibrillation (Henriksson et al. 2007; Pääkkö et al. 2007). It is well-known that endoglucanase activity is selective to β-1,4-glucosidic bonds in cellulose (Liu et al. 2009). Earlier work also describes that the endoglucanase activity preferentially takes place at dislocations along the fibre (Ander et al. 2008; Thygesen et al. 2011). Such dislocations comprise of only a small portion of the total accessible surface of the fibre and hence, might get saturated at a certain enzyme loading. Thus, an increase in endoglucanase dosage above the saturation point might not be effective (Gourlay et al. 2018). On the other hand, exoglucanases, such as cellobiohydrolases are known to attack the cellulose chains from either end, releasing cellobiose units (Quinlan et al. 2010). The presence of lignin and hemicelluloses has been found to reduce the extent of cellulase activity due to inaccessibility of cellulose for the enzyme to bind upon (Igarashi et al. 2011; Laureano-Perez et al. 2005; Mosier et al. 2005). Hence, a combination of cellulases or hemicellulases,

acting synergistically, is typically required to achieve efficient hydrolysis via a purely enzymatic route (de Campos et al. 2013). As an alternative route, mechanical refining of cellulose before enzymatic treatment can be used to increase the number of dislocations and the available surface area of fibres for enzymatic action (Gao et al. 2015; Hoeger et al. 2013).

Multicomponent cellulase cocktails composed of a mixture of endoglucanases and exoglucanases (cellobiohydrolases) to obtain CNMs were studied by Siqueira et al. (Siqueira et al. 2010, 2011). Hu et al. termed the enzymes/proteins, such as xylanases and lytic polysaccharide monooxygenases (LPMO), which enhance the action of cellulases, as 'accessory enzymes' and reported the use of those in pulp fibrillation (Hu et al. 2013, 2018). In another work, de Campos et al. reported the use of endoglucanase along with an accessory pectinase and hemicellulases (de Campos et al. 2013).

In most studies, the enzymatic treatment has been followed by mechanical fibrillation processes such as sonification (de Campos et al. 2013; Hu et al. 2018), homogenization (Henriksson et al. 2007), and fluidization (Pääkkö et al. 2007) to obtain nanoscale fibres. However, all three processes are highly energy intensive, requiring material dilution to low consistencies, typically below 5%, in order to yield fine fibres. The use of low consistency CNMs increases logistics costs and limits applications in areas that demand low water amount during processing. For instance, the presence of water in conjugation with hot-melt polymers during compression molding, injection molding, and film extrusion limits CNMs use as reinforcement in composites. In food packaging applications, a considerable obstacle for use of CNMs as a gas barrier film or coating is the required excessive drying capacity during processing, which inhibits high-speed production (Kumar et al. 2016).

Several studies have addressed the need to overcome the obstacles related to the high energy consumption of CNM manufacturing and low solids content of the resulting material. Mechanical fibrillation of never-dried bleached kraft pulp fibres was demonstrated by Ho et al. (2015) using a twin-screw extruder (TSE) where the resultant product was moist CNF powder at 33–45% solids. However, the process faced practical challenges due to excessive heat generation in the TSE after 10 passes leading to excessive depolymerization of the cellulose chains and a loss in crystallinity. Moreover, the redispersibility of the CNF powder in water might be challenging due to fibre hornification. Baati et al. (2017) also used a TSE to fibrillate pulp fibres after TEMPO-mediated oxidation. The extrusion process yielded strong CNF gels at up to 10% solids with carboxyl content ranging from 300 to 900 μmol/g. In a separate work, Rol et al. (2017) utilized a TSE to demonstrate the fibrillation of enzymatically pretreated bleached kraft pulp to produce a paste-like material at approximately 20% solids. The energy consumption during the production of CNFs at 20% solids using TSE (7 passes) was approximately 5000 kWh/t which was 63% lower than production using a grinder.

Apart from the TSE-based technologies, an enzymatic approach named high-consistency enzymatic fibrillation of cellulose (HefCel) was developed at VTT (Hiltunen et al. 2015). The HefCel method uses a reactor equipped with a sigma-type mixer that enables precise temperature control, uniform mixing of the enzyme cocktail with the cellulose substrate and employing fibre–fibre friction to obtain fibrillation in synergy with the enzymatic action. After all unit operations, a high-consistency fibrillated material can be produced at 10–25% solids. The energy demand for the HefCel process was calculated to be roughly 900 kWh/t in our previous investigation (Lehmonen et al. 2017). Thus, the HefCel method has a lower energy consumption compared to other manufacturing methods such as refining, grinding, homogenization, ball milling, and extrusion because it only requires a simple mixing process.

It is evident that high-consistency fibrillation leads to advantages such as low production costs, energy savings, easier logistics and better suitability of CNF for industrial applications. Previous studies have focused on optimizing process parameters, such as TSE screw geometry, shear profile, and number of TSE passes, for production of high-consistency materials (Ho et al. 2015; Rol et al. 2017). However, there is still a lack of information regarding the effect of varying factors such as enzyme dosage and the role of cellulose substrate composition on the properties of the resultant material in high-consistency processes. Understanding such a relationship could pave the ways to produce CNMs with properties tuned for optimal performance in specific applications.

The present work investigates the structure–property relationship in fibrillated cellulose materials

produced using the HefCel process. For this, the effects of enzyme dosage and raw material composition on the morphological and rheological properties of the resultant fibrillated cellulose material (hereafter termed as HefCel grades) were studied. Three different wood pulps were used as raw materials and three different enzyme dosages were studied for each pulp, giving nine grades of fibrillated cellulose materials at 17–23% solids content. To demonstrate the performance of the grades in a typical application, films were casted using dilute suspensions and were characterized for their mechanical properties.

Experimental section

Materials

Three different bleached kraft pulps were used in the study, namely once-dried softwood pulp, never-dried softwood pulp, and once-dried hardwood pulp. The softwood pulps were procured from Metsä Fibre Bioproduct Mill (Äänekoski, Finland). The never-dried pulp was received at ca. 37% solids content and the once-dried pulp at 95% solids. Hardwood pulp was obtained in once-dried state from a Finnish pulp mill. All pulps were bleached at the production site. The used enzyme cocktail (EcoPulp Energy, AB Enzymes, Finland) was a multicomponent cellulase with both endo-and- exoglucanase activity and minor background hemicellulase activities.

Fibrillated cellulose production

Fibrillated cellulose suspensions were produced from pulps using HefCel technology developed at VTT. Once-dried pulps were slushed in water at 25% consistency, and the pulp suspension was then transferred to a reactor equipped with a temperature controller and a two-shaft sigma-type mixer (Winkworth Machinery Ltd., UK) as shown in Fig. 1. The never-dried pulp was used as such. The enzyme mixture was dosed to the pulp suspensions in the reactor while keeping the mixing speed constant at 25 RPM and the temperature at 70 °C. The enzyme type, dosage amount, and treatment time are parameters critical to the final HefCel quality. Three different enzyme dosage levels viz. 6, 8, and 10 mg/g (on dry fibre mass) were used with each type of pulp to observe the effect of enzyme dosage level on the resultant HefCel quality. These enzyme dosage levels have been selected based on our prior experience with the HefCel process, where all three levels lie within the operational window of the process. Further details concerning the HefCel process have been reported elsewhere (Pere et al. 2020).

The treatment time was fixed at 6.5 h for all samples. After 6.5 h, the enzyme activity was stopped by increasing the temperature in the reactor to 90 °C for 30 min. Subsequently, the obtained HefCel was washed with deionized water to remove any remaining enzyme. Water added during the washing stage was then filtered out from the HefCel under mild vacuum to obtain a final consistency of approximately 20%. The obtained materials were stored at 4 °C until use in experiments. The wash water from the process was analyzed for carbohydrates using the dinitrosalicylic acid (DNS) assay of reducing sugars as suggested by Rahikainen et al. (2020) and originally developed by Sumner and Noback (1924).

Characterization of HefCel

A high speed mixer (Dispermat^{TM} LC) was used to make dilute suspensions from the high consistency HefCel suspensions. The suspensions were homogenized for at least 15 min at 2000 RPM before performing any experiments. pH measurements were performed directly on the high consistency HefCel suspensions obtained after the filtration stage using a standard portable pH meter (Mettler Toledo SG2). The conductivity of the HefCel suspensions, diluted to 2% consistency, was measured at room temperature using a Jenway 4510 conductivity meter.

Carbohydrate analysis and molar mass measurements

To determine the carbohydrate composition, the source pulps and fibrillated samples were hydrolyzed with sulphuric acid and the resulting monosaccharides were determined by High-performance anion exchange chromatography (HPAEC) with pulse amperometric detection (Dionex ICS 3000A equipped with CarboPac PA-1 column) according to the NREL method (Sluiter et al. 2012; Pettersen 1991). The polysaccharide content in the samples was calculated from the corresponding monosaccharides using an

Fig. 1 The setup for HefCel production (left), inside view of the mixer after opening the mixer lid (right)

anhydro correction of 0.88 for pentoses and 0.9 for hexoses.

For the molar mass measurements, solid samples were dissolved in DMAc/8% LiCl according to the solvent exchange method described by Berggren et al. (2003). This method includes activation of the sample with water, solvent exchange with methanol and DMAc, followed by ethyl isocyanate derivatization assisted dissolution into DMAc/8% LiCl. After complete dissolution, the samples were diluted with DMAc providing final LiCl concentration of 0.8% as in the eluent. In all cases, the samples were filtered (0.45 µm mesh) before the measurement. For all samples, size exclusion chromatography (SEC) measurements were performed using PLgel MiniMIX A columns with a precolumn in DMAc/0.8% LiCl eluent (0.36 ml/min, T = 80 °C). Two parallel samples of each pulp and HefCel were studied.

Fiber analysis

The morphology of the HefCel fibres were investigated with a Kajaani FibreLab analyzer (Metso Automation, Kajaani, Finland) equipped with FibreLab 4Core. Fibre samples (approx. 0.1 g oven-dry mass) were taken to the automated fibre analysis device to measure fibre parameters such as fibre length (weight-weighted average fibre length), curl, kinks, and fines content.

Morphology

Optical microscope (Olympus BX61 equipped with WH4X-H eyepieces, fluorite objectives and a ColorView 12 camera) was used to analyze the HefCel samples. To obtain sufficient contrast in the images, each sample was dyed with 1% Congo red solution in 1:1 ratio by volume before imaging. Atomic force microscopy (AFM) was performed to analyze the nanoscale fibril fraction. HefCel samples were diluted to 0.5 wt.% solids using deionized water and centrifuged (5804 R Centrifuge, Eppendorf AG) at 10,400 RPM for 45 min. Then approximately 5 ml of the supernatant was taken for spin coating. AFM (MultiMode 8 Scanning Probe Microscope, Bruker AXS Inc.) was used to analyze the surface topography of spin-coated samples on polyethyleneimine-coated SiO_2 wafers. Tapping mode in air and silicon cantilevers (NSC15/ALBS, MikroMasch) were used to scan 3 × 3 μm^2 and 5 × 5 μm^2 surface areas. At least three sample areas were imaged and flattening was used in image processing by using Nanoscope Analysis 8.15 software.

Rheology and water retention

All rheology measurements were performed using a stress-controlled rotational rheometer Physica MCR 301 (Anton Paar GmbH). Shear flow measurements were performed using a Couette-type smooth-walled concentric cylinder geometry. The diameters of the inner and the outer cylinder were 27.00 mm and 29.29 mm respectively, and the vertical gap between the two cylinders was kept at 1 mm. For all measurements, samples were pre-sheared at 100 s^{-1} for 60 s and were then left idle for 120 s before starting data recording, according to the protocol suggested by

Naderi et al. (Naderi and Lindström 2016). This protocol ensures homogeneity in the sample.

The shear rate sweeps were performed in the interval of 0.1–1000 s^{-1} and data was collected at 40 different points with 10 s measurement duration per point. Oscillatory measurements were performed using a vane-and-cup geometry (vane span: 22 mm, cup diameter 29.29 mm) to avoid wall-slip effects on measurements results, as suggested by Mohtaschemi et al. (Mohtaschemi et al. 2014). Oscillatory strain sweeps were performed in order to determine the linear viscoelastic (LVE) region with strain ranging from 0.1–100% while the frequency was kept constant at 10 rad/s. The strain sweeps were followed by frequency sweeps in the range of 0.1–100 Hz, while keeping the strain within the LVE region of the sample. Three parallel measurements were conducted. Yield stress for the suspensions was calculated using the strain sweep data. The shear stress at which the value of storage modulus dropped to 90% of its initial value was defined as the yield stress.

Static gravimetric dewatering of HefCel suspensions was studied using Åbo Akademi Gravimetric Water Retention (ÅA-GWR) method, originally developed by Sandås et al. (1989). Dewatering was studied at four different concentrations viz. 2, 5, 7, and 10% for each type of HefCel. For measurement, 10 ml of sample was inserted into a measurement cylinder of known diameter, placed above a 5 µm polycarbonate membrane (GE Water & Process Technologies, USA) and backed by multiple sheets of absorbent blotter papers of known mass. After a fixed duration of 15 s of placing the sample into the measurement cylinder, the cylinder was sealed and constant air pressure of 50 kPa was applied for 90 s. After depressurization, the sample was kept in contact with the membrane and blotter papers for 15 s and weighed. GWR value represents the amount of water released by the suspension per unit area. The reported results are an average of three parallel measurements.

Film casting and testing

In order to study the self-assembling behavior of the HefCels, standalone films were prepared by casting a calculated amount of 2 wt.% HefCel suspension in Petri dishes placed on a horizontal surface. The target basis weight was 50 g/m^2. Five parallel samples were prepared for each grade of HefCel. The films were dried and tested in a conditioned environment, regulated at 23 °C and 50% relative humidity (RH). Basis weight of the films was measured by weighing a film sample of known size. Dry film thickness was measured using an L&W Micrometer 051 (Lorentzen & Wettre AB) following the TAPPI T411 standard. Tensile tests were performed using a Lloyd LS5 materials testing device (AMETEK Inc., USA) equipped with a load cell of 100 N. The strain rate

Table 1 Composition of the source pulps and the prepared fibrillated materials

Sample code	Enzyme dosage (mg/g)	Glucose (%)	Xylan (%)	Cellulose (%)	Liberated reducing sugars (%)
SW ND	0	82.9 ± 1.3	7.8 ± 0.2	71.3 ± 1.1	–
SW ND6	6	81.3 ± 0.6	7.7 ± 0.2	69.6 ± 0.5	9.7
SW ND8	8	81.5 ± 2.0	7.7 ± 0.2	69.8 ± 1.7	10.3
SW ND10	10	77.4 ± 3.8	7.3 ± 0.3	66.3 ± 3.3	14.0
SW 1D	0	82.6 ± 1.2	8.9 ± 0.2	71.5 ± 1.1	–
SW 1D6	6	81.8 ± 0.5	9.3 ± 0.1	70.6 ± 0.4	9.4
SW 1D8	8	81.0 ± 0.9	9.3 ± 0.1	69.9 ± 0.8	11.5
SW 1D10	10	81.2 ± 0.4	9.3 ± 0.1	70.0 ± 0.3	13.5
HW 1D	0	71.4 ± 2.2	19.6 ± 0.7	63.6 ± 1.9	–
HW 1D6	6	70.9 ± 0.5	19.6 ± 0.1	63.1 ± 0.4	9.7
HW 1D8	8	71.6 ± 0.4	19.7 ± 0.2	63.7 ± 0.3	12.6
HW 1D10	10	71.3 ± 0.4	19.7 ± 0.2	63.4 ± 0.3	13.9

Abbreviations: Once-dried hardwood (HW 1D), Once-dried softwood (SW 1D), Never-dried softwood (SW ND). The number after the pulp name indicates the enzyme dosage in mg/g, based on dry fibre mass. Reducing sugars were measured in the filtrate after washing the produced HefCel grades and are reported as mass percentage of the total dry pulp mass used

was set to 10 mm/min and the gauge length was 50 mm. Tensile strength, Young's Modulus, and Strain at Break (SaB) are reported as a mean of five measurements per sample.

Results and discussion

The present work studies the effect of enzyme dosage and raw material composition on the properties of the resultant fibrillated cellulose material from the HefCel

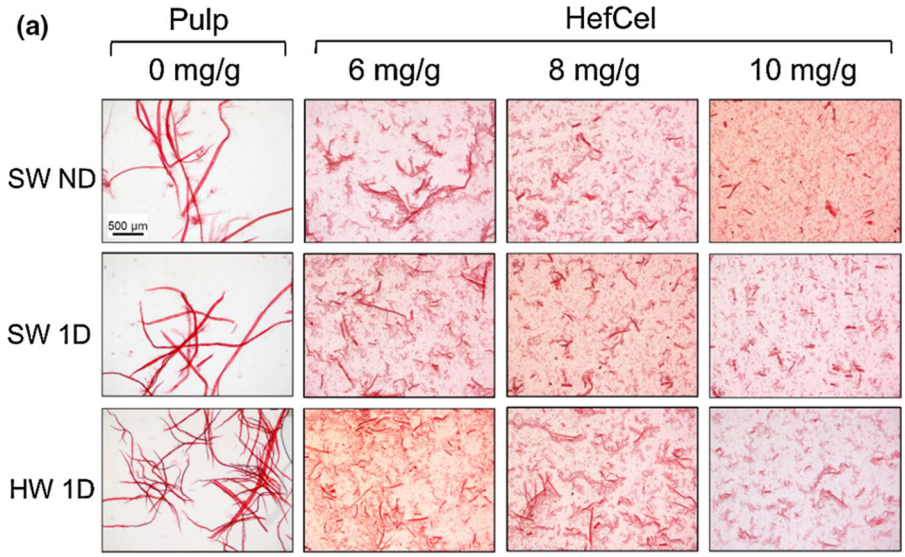

Sample	SW ND	SW ND6	SW ND8	SW ND10	SW 1D	SW 1D6	SW 1D8	SW 1D10	HW 1D	HW 1D6	HW 1D8	HW 1D10
Fibre length (mm)	1.85	0.22	0.16	0.19	1.94	0.13	0.18	0.18	1.04	0.23	0.23	0.10
Fibre width (µm)	27.1	16.8	15.1	13.7	25.1	17.1	15.5	14.1	20.8	16.4	15.4	15.6

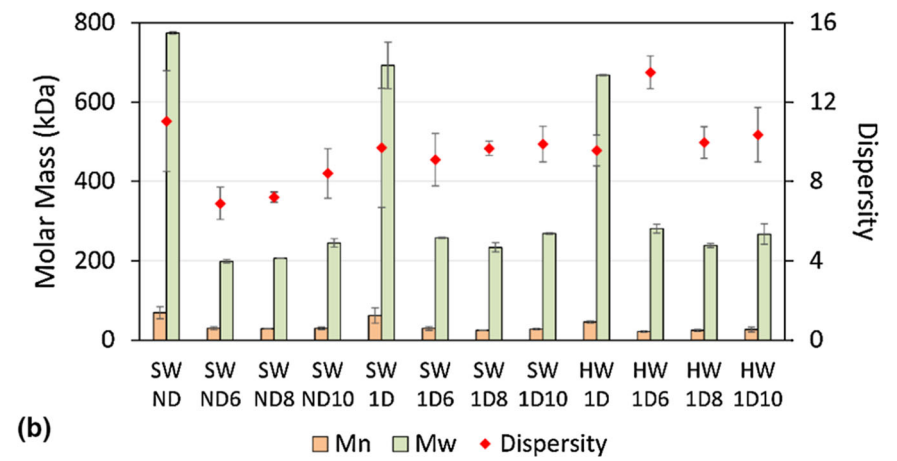

Fig. 2 **a** Images of the source pulps and HefCel suspensions taken using an optical microscope. The scale bar denotes 500 µm length. The table underneath enlists the length-weighted average fibre length and mean diameter for the same samples measured using an optical analyzer (standard deviations can be found in the Online Resource 1. **b** Average molar mass and dispersity of the same samples. Mn = number average molecular weight, Mw = weight average molecular weight and dispersity = Mw/Mn

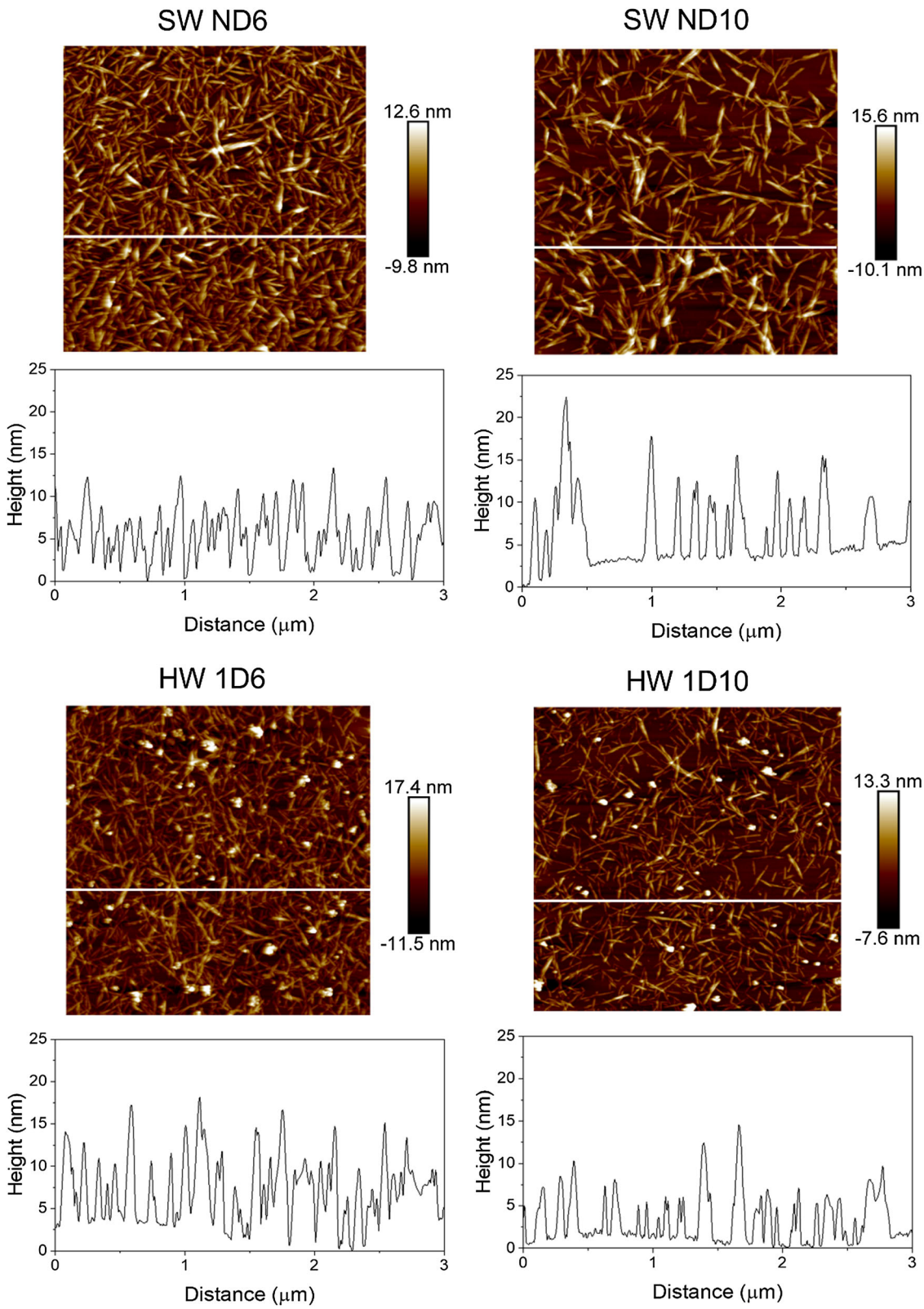
SW ND6
12.6 nm
-9.8 nm
Height (nm)
Distance (μm)
SW ND10
15.6 nm
-10.1 nm
Height (nm)
Distance (μm)
HW 1D6
17.4 nm
-11.5 nm
Height (nm)
Distance (μm)
HW 1D10
13.3 nm
-7.6 nm
Height (nm)
Distance (μm)

◀**Fig. 3** AFM images of four HefCel grades taken from an area of 3 × 3 μm^2. The horizontal lines over the images indicate the lines along which the fibril width was analyzed. The graphs underneath each image show the fibril width profile (denoted as height) across the image along the marked line

process. Three different wood pulps were used as raw materials and three different enzyme dosages were studied for each pulp, giving nine grades of fibrillated cellulose (termed as HefCel grades) in total. All production process parameters were kept constant except for the enzyme dosage level. Table 1 lists all the samples with their abbreviated codes used in further discussion along with their carbohydrate composition, and liberated reducing sugars content in the wash water obtained from each grade. Abbreviations to the sample codes are listed in the table footnote. The pH of all HefCel samples was found to be in the range of 5–6. The used enzyme cocktail exhibits the highest activity level in the same pH range and thus, the measurement ensured that the fibrillation was done under optimum conditions. Electrical conductivity values were found to be quite low in all samples, below approximately 20 μS/cm, which was an indicator of no additional free ions being released to the suspensions during the production process.

Table 1 lists glucose, xylan, and cellulose content of the source pulps and the HefCel samples. The fairly constant glucose and cellulose content in the source pulps and in the HefCel grades derived from those respectively, indicates that the enzymatic hydrolysis occurred randomly in the cellulose chains and the cleaved cellulose chains were not fully converted to soluble sugars. Additionally, it shows that the chemical composition of the pulps was not significantly altered during enzymatic hydrolysis. The residual sugar analysis done on the filtrate after washing the produced HefCel grades indicates the loss of raw material in form of soluble sugars during processing. A common trend can be observed for all raw materials: as the enzyme dosage increased, the amount of soluble sugars in the filtrate also increased, suggesting more hydrolysis on the reducing end and ultimately, losses in process yield. The hardwood pulp and the hardwood-derived HefCel grades were found to contain a high amount of xylans, which is typical for hardwood fibres. The used enzyme cocktail had only minor background hemicellulase activity and thus, the amount of xylans in the initial pulps and the respective HefCel grades did not differ much. The full carbohydrate composition data can be found in the supplementary information (Online Resource 1).

Fibre characterization

The extent of enzymatic degradation of the fibres was studied by four different methods, viz. optical microscopy, an optical fibre analyzer, molar mass measurement, and AFM imaging. Figure 2 (a) illustrates a compilation of optical microscope images for all three pulps and nine grades of HefCel, along with their mean length-weighted fibre length and mean fibre width. The optical microscope images show the micro-sized fraction of the HefCel materials and the fibre size analysis done via FibreLab is only valid for this fraction. The enzymatic treatment causes a significant reduction in the fibre length, whereas the fibre diameter was not much affected since some fibres were not fibrillated during the process. Such behavior has been previously reported for monocomponent endoglucanase treatment on cellulose substrates (Gourlay et al. 2018). An interesting observation is that the hydrolysis action was not a direct function of enzyme dosage but rather dependent on the raw material composition. The increase in enzyme dosage did not universally correlate with the change in aspect ratio of the fibres. For instance, the lowest aspect ratio of 6.4 was found in the HW 1D10 sample, whereas in the case of softwood-derived grades, the lowest aspect ratio of 7.3 was found in the SW 1D6 sample. Since the HefCel method takes advantage of the interfibre friction generated by mixing at high consistency to unravel fibrils in combination with cellulase action, the HefCel grades had lower fibre widths than source pulps. The fines content in all HefCel grades was found to be more than 90% whereas the softwood pulps contained roughly 25% fines and the hardwood pulp contained approximately 10% fines.

As expected, the softwood pulp fibres had a higher aspect ratio than the hardwood counterparts, however, the softwood-derived HefCel grades showed a lower aspect ratio than the hardwood-derived grades. This peculiar observation can be explained by the presence of a high amount of hemicelluloses in the hardwood pulp that affects the hydrolysis behavior. Hemicelluloses, such as xylan, restrict the interaction of enzymes with the cellulose chains and consequently, decrease

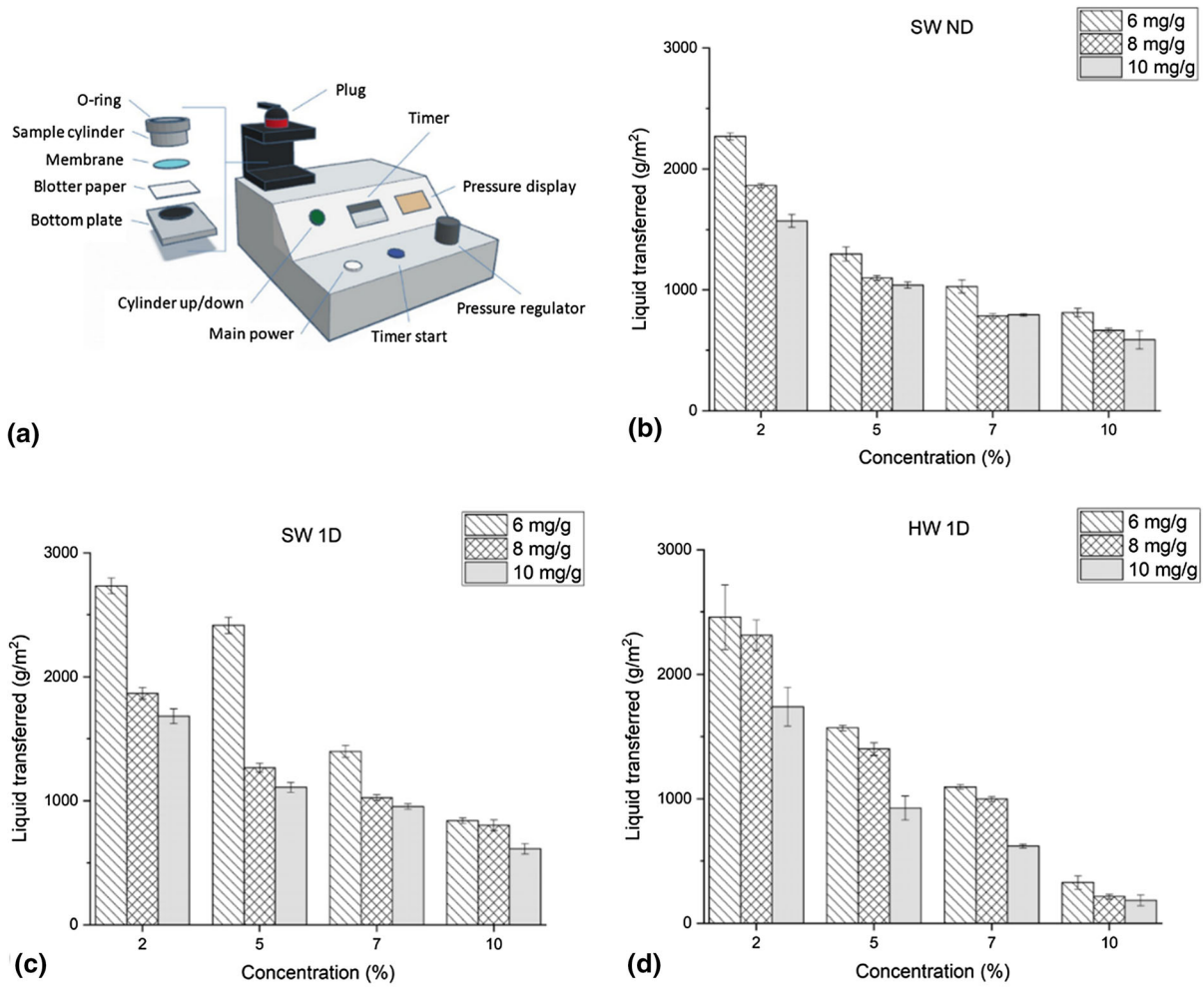

Fig. 4 **a** Schematic description of the setup for the ÅA-GWR measurements. Dewatering values, measured as liquid transferred to the blotter papers, as a function of concentration for HefCel suspensions obtained from SW ND (**b**), SW 1D (**c**), and HW 1D (**d**) pulps

the extent of enzymatic action (Igarashi et al. 2011; Penttilä et al. 2013; Zhang et al. 2012). Thus, almost similar fibre dimensions were observed for the hardwood-derived HefCel grades HW 1D6 and HW 1D8. In general, cellulase action can be inhibited by the presence of any non-cellulosic material in the raw material, such as, lignin, ink pigments, glues, or resins, which restrict the enzyme access to cellulose. It must be noted that the optical methods were only used to study the micro-sized fraction of the HefCel materials.

The results from the optical measurements were found to be in agreement with the SEC results. The average molar mass of cellulose chains in the fibrillated suspensions was found to be much lower than the source pulps (Fig. 2b). Moreover, the increase in enzyme dosage, while keeping the treatment duration and conditions constant, did not lead to a decrease in the average molar mass. A similar observation has been reported in earlier work by Gourlay et al. (2018) where it was postulated that beyond a certain enzyme loading, the dislocations on the fibre surface get saturated and the endoglucanase action is restricted due to inaccessibility to the substrate. Such explanation holds merit as the preferential action of endoglucanase on dislocations on cellulose fibres along the fibre length is well-described in earlier work (Hidayat et al. 2012, 2015; Thygesen et al. 2011).

Since the optical analyses dealt only with the microscale fraction of the HefCel grades, AFM imaging was performed to analyze the nanoscale fibril

fraction. The presence of nanoscale fraction, separated via centrifugation, indicated the occurrence of fibrillation of pulp fibres during processing. Figure 3 shows AFM images comparing the lowest and the highest enzyme dosages for both softwood and hardwood derived HefCel grades. The fibrils have high aspect ratios, a "curly" appearance, and diameters in the range of 5–20 nm. For instance, at an average length of 1 µm, 5–20 nm diameter corresponds to an aspect ratio of 50–200. Similar studies have reported that CNF produced via the enzymatic route using a twin screw extruder had an average diameter of 25.4 ± 7.1 nm (Rol et al. 2017).

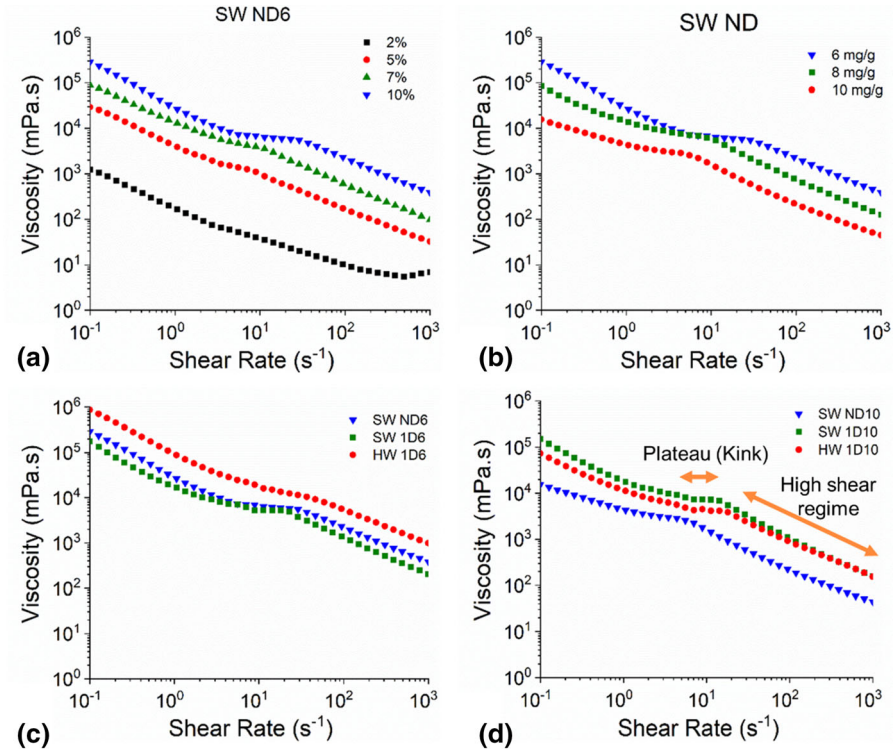

(e)

Enzyme dosage →

	6 mg/g					8 mg/g					10 mg/g				
	Consistency (%)					Consistency (%)					Consistency (%)				
	2	5	7	10	m	2	5	7	10	m	2	5	7	10	m
SW ND	0.45	0.26	0.20	0.25	3.36	0.53	0.41	0.23	0.16	3.82	0.68	0.41	0.31	0.21	3.93
SW 1D	0.47	0.23	0.20	0.17	3.36	0.73	0.34	0.28	0.18	4.31	0.62	0.19	0.18	0.11	4.20
HW 1D	0.43	0.27	0.25	0.28	4.09	0.49	0.27	0.23	0.22	3.70	0.37	0.26	0.21	0.22	2.75

Power law equation: $\tau = K.\dot{\gamma}^n$ and $\mu \propto c^m$

Fig. 5 **a** Forward shear rate ramps for SW ND6 sample at consistencies of 2, 5, 7, and 10%. **b** Shear rate ramps for HefCel grades derived from SW ND pulp using 6, 8, and 10 mg/g enzyme dosage. **c** Effect of changing pulp type on the viscosity of grades containing 6 mg/g and **d** 10 mg/g respectively. Subfigures (**b**), (**c**) and (**d**) show curves for labelled samples at 10% consistency. **e** The table below lists the power law indices (n) for each flow curve in the high shear regime and the parameter m denoting the correlation between suspension viscosity and consistency calculated at shear rate of 1 s^{-1}

Water retention and rheology

Water retention values of HefCel suspensions were measured using the ÅA-GWR method. ÅA-GWR is an indirect measurement method where static gravimetric dewatering of a material is studied under mild overpressure. The method was originally developed to study water retention of paper coating colors and is relevant for studying the dewatering of cellulosic materials for applications in thin-film structures such as self-standing films and coatings, where the material layer lies in contact with an absorbent substrate (Dimic-Misic et al. 2013; Kumar et al. 2016). The results from the measurements are illustrated in Fig. 4, where a higher amount of liquid transferred to the blotter paper indicates lower water retention by the material. For the used measurement setup, a water retention value of 3000 g/m^2 corresponded to 20% dewatering of the suspension when calculated on the basis of total water present in the suspension.

All HefCel suspensions, quite expectedly, exhibited an increasing trend in water retention as the concentration of the suspension was increased. The lower amount of water present in more concentrated suspensions directly correlated to the lower dewatering tendency. HefCel grades derived from never-dried softwood pulp were observed to retain water better than their counterparts derived from once-dried softwood pulp at all tested concentrations and at all enzyme dosage levels. This behaviour can be understood to be resulting from hornification of fibres in the once-dried pulp. The lower water retention of hornified fibres compared to virgin fibres due to a lower number of free hydroxyl groups available for hydrogen bonding with water molecules is well-known (Fernandes Diniz et al. 2004). For all HefCel grades, an increase in the enzyme dosage level resulted in lower dewatering. Dewatering rate is associated with the rate of water diffusion through the filter cake formed on top of the absorbent paper. Higher water retention was expected to be resulted from a combined effect of high degree of fibrillation, increasing the fibre surface area and amount of fines in the system, which allow the formation of a dense filter cake.

Fibrillated cellulose materials are known to possess a complex rheology. CNM suspensions, even at low consistencies of 1–3%, possess high yield stress but also exhibit a steep shear-thinning behavior (Hubbe et al. 2017a, b). Such behavior is found to be more prominent in fibrillated CNM grades, such as CNFs than in CNCs due to physical entanglement between fibrils. Applications of fibrillated cellulose materials in coatings, 3D printing and rheology modification require overcoming the challenges associated with high yield stress and viscosity along with the typical low solids content. For instance, Kumar et al. used a slot-die to shear a 2% CNF suspension in order to apply a uniform coating layer on paperboard moving at speed of 3 m/min (Kumar et al. 2016). Applying CNF coatings was not straightforward using conventional methods like blade and rod coating at such low speeds and the shear-thinning (power law index 0.2) in the slot was crucial for the process. Even if the coating was made possible with such high viscosity gels (ca. 80,000 mPa.s at 1 s^{-1} for 2% CNF suspension), high-speed processing was still limited by the excessive drying demand. In 3D printing applications, Klar et al. (2019) described that the typical low consistency of CNF suspensions was detrimental to shape fidelity of 3D printed structures due to high shrinkage upon drying. Thus, a fibrillated cellulose material which possesses low viscosity while maintaining a pseudoplastic nature, used at high consistency (5–15%), could be useful for applications in coatings and 3D printing. In the current work, the shear viscosity of the HefCel grades was studied as a function of suspension consistency, ranging from 2 to 10%.

In the present study, the produced HefCel grades had a wide fibre size distribution, ranging from unfibrillated microsized fibres to nanoscale fibrils. Due to such mixed size distribution, the fibre network entanglement, which governs the suspension viscosity, varied greatly. The HefCel grades were found to have much lower viscosities than typical CNMs (Fig. 5). For instance, viscosities of 2% CNF suspensions at shear rate of 1 s^{-1}, were measured to be approximately 60,000 mPa s by Turpeinen et al. (2020) and 80,000 mPa s by Kumar et al. (2016). For the HefCel grades, the viscosities at 2% solids were several orders of magnitude lower and fell in the range of 20–200 mPa s. However, viscosities comparable to CNFs was found for several HefCel grades at 7% and 10% solids. Hence, these HefCel grades could prove suitable in film forming, coating and printing applications without the employment of ultra-high shear rates and could reduce the drying energy requirements significantly. This is evident from the fact that a film (at same basis weight) made from a

material at 10% solids contains 82% less water as compared to one made at 2% solids.

The viscosity of HefCel suspensions generally appeared to decrease with increasing enzyme dosage. The only outlier to this trend was the SW1D10 sample, for which the viscosity seemed to increase when compared to the SW1D8 sample (see supplementary information for data (Online Resource 1)). There was no significant difference in the average fibre dimensions upon varying the enzyme dosage, however, the difference in viscosity was substantial. No straightforward correlation between the fibre aspect ratio and viscosity of the suspensions could be identified. A possible explanation of the decrease in the suspension viscosity with increasing enzyme dosage could be the one described by Gourlay et al. who reported in two separate works that the surface of cellulose fibres contained isolated and highly accessible cellulosic strands, which contributed towards interfibre entanglement and increased the suspension viscosity (Gourlay et al. 2015). In a later work, it was reported that the 1 mg/g enzyme dosage for 30 min resulted in a 75% viscosity drop (compared at 0.1 s^{-1}) while the aspect ratio of fibres decreased by only 5% (Gourlay et al. 2018). This behavior was attributed to the hydrolysis of the accessible cellulosic strands, which lowered the possibility of interfibre entanglement. Thus, in these studies as well, fibre dimensions remained almost similar but a drop observed in viscosity could be attributed to the same phenomenon.

Recently, Koponen (2019) prepared a review on the dependency of viscosity (μ) and yield stress (τ_y) of CNFs on suspension consistency (c). Rheology data for a wide range of CNF grades was analyzed and it was shown to obey similar scaling laws when fitted to the power law equation, $\tau = K.\dot{\gamma}^n$, where τ is shear stress, K is consistency index, $\dot{\gamma}$ is shear rate, and n is the flow index (power law index). The data was found to universally fit well to the power law relationship and the following correlations were derived, (i) $n \propto c^{-0.43}$, (ii) $K \propto c^{2.43}$, and (iii) $\tau_y \propto c^{2.26}$. Clearly, rheological parameters were highly dependent on the suspension consistency. It must be noted the above relationships were derived from rheology data of suspensions having consistencies of 0.01–7% solids, but most of the data was in the consistency range of 0.5–3.

In the present work, following a similar methodology as described by Koponen (2019), the shear flow data for the HefCel grades at different consistencies was fitted to the power law equation $\tau = K.\dot{\gamma}^n$. Values for K and n were derived from the power law fits and the dependence of both parameters on suspension consistency was analyzed. All values reported for the fitting parameters correspond to models with correlation (R-squared) values greater than 0.99 with the experimental curve.

The forward shear rate ramps illustrated in Fig. 5 show the presence of a 'kink' in the curves at shear rates of approximately 10 s^{-1}. Such a viscosity plateau is a typical feature in shear flow curves for fibrillar CNMs and has been described frequently in literature (Hubbe et al. 2017a, b). Karppinen et al. (2012) and Saarinen et al. (2014) imaged the flow of CNF suspensions at 0.1–2% and 0.5–1% consistencies respectively, and showed that soft fibrillar flocs are present in the suspensions at low shear rates. As the shear rate increases, the flocs grow in size, thus offering a greater resistance to the flow, increasing the viscosity, and leading to the plateau in the flow curve. With further increase in shearing, the flocs get broken and fibrils get aligned with flow streamlines, causing a rapid decrease in viscosity subsequent to the plateau region. Hence, due to microstructural changes in the suspensions, the shear flow curve follows different power law models in different shear rate regimes before and after the 'kink.

The flow indices shown in Fig. 5e are calculated for the high shear rate regime (after the plateau) in each suspension. All values for the consistency index and the flow indices for the low shear rate regime can be found in the Online Resource 1. The power law indices decreased with increasing suspension consistency, denoting a higher shear-thinning character at higher consistency but the drop tended to saturate in some samples beyond 5% solids. The increase of shear thinning tendency, manifested in decrease of the flow index, with an increasing solids content has been reported previously (Schenker et al. 2018). In a separate work, Schenker et al. (2019) offered a possible explanation underlying this behavior where they suggested that at high consistencies, the attractive interactions between fibres are more pronounced than at low consistencies due to the lower distance between fibres. This causes higher aggregation at high consistencies which, when broken down under shear, leads to enhanced pseudoplastic behavior.

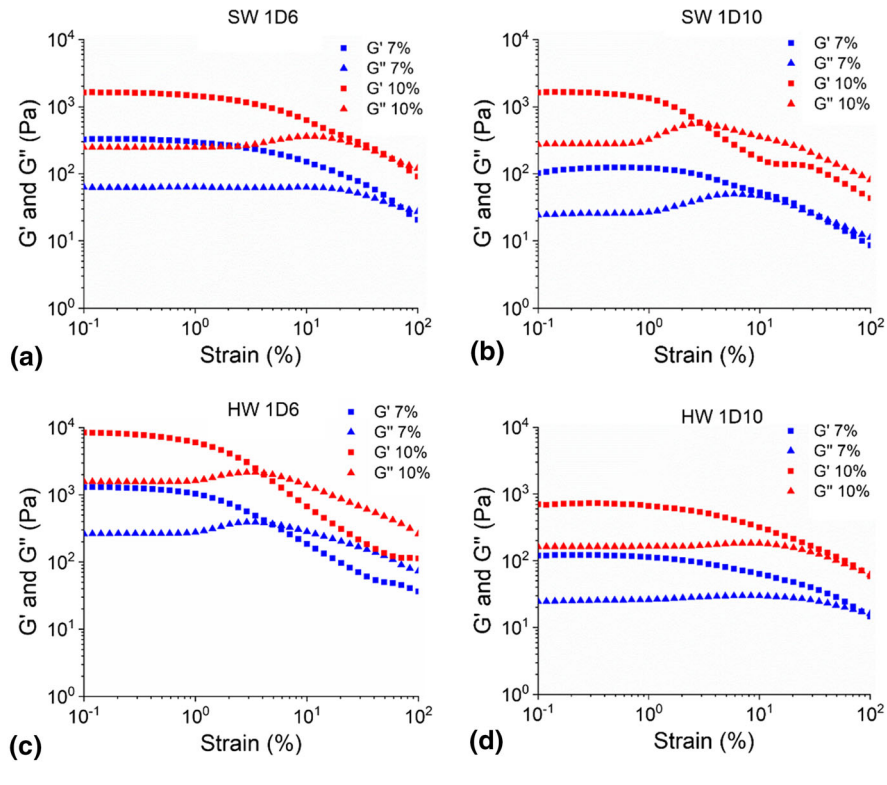

(e)

Enzyme dosage

τ_y (Pa)	6 mg/g		8 mg/g		10 mg/g	
	Consistency (%)		Consistency (%)		Consistency (%)	
	7	10	7	10	7	10
SWND	4.3 ± 0.6	17.7 ± 2.6	0.8 ± 0.1	7.0 ± 0.3	0.3 ± 0.1	6.0 ± 1.9
SW1D	3.9 ± 1.1	14.6 ± 0.6	0.2 ± 0.1	4.6 ± 0.4	3.5 ± 0.9	10.8 ± 0.3
HW1D	7.4 ± 1.4	21.4 ± 6.3	3.5 ± 1.0	13.6 ± 2.9	2.2 ± 0.6	17.6 ± 6.7

Fig. 6 **a** Strain sweeps at 7 and 10% consistencies for SW 1D6 and **b** SW 1D10 samples. Similarly, subfigures (**c**) and (**d**) show strain sweeps for HW 1D6 and HW1D 10 samples respectively. Curves for all other samples can be found in supplementary information. Subfigure (**e**) shows the yield stress values for the HefCel samples

The dependence of suspension viscosity on the consistency was analyzed in terms of the parameter *m*, which was calculated using the relation $\mu \propto c^m$ as described earlier by Hubbe et al. (2017a, b). Figure 5e shows that the viscosity was found to be strongly dependent on the consistency with *m* values ranging from 2.75 to 4.31 for different HefCel grades. In an earlier work, this value was derived to be approximately 2.5 for fibrillar CNMs, where the analysis was limited to the consistency range of 0.3–3% (Koponen 2019). It must be noted herein that the parameter *m* is not unique but dependent on the shear rate. Koponen (2019) modeled the value of *m* at various shear rates and the value of 2.5 was calculated at shear rate of 1 s^{-1} and for comparison, the values have been calculated at the same shear rate in the current work.

All the HefCel grades had extremely low viscosity at 2% solids. Thus, at shear rates of 200–1000 s^{-1}, secondary flows (Taylor vortices) were generated, causing flow resistance and therefore, the viscosity seemed to increase at high shear rates. Therefore, the data at 2% solids at high shear rates is not accurate but still has been presented to show the lower limit of consistency for such measurements. This data was also

Table 2 Results from tensile testing of casted films

Sample	Basis weight (g/m^2)	Film density (kg/m^3)	Tensile strength (MPa)	Young's modulus (GPa)	Strain at break (%)
SW ND6	48.9 ± 0.3	1083 ± 7	45.7 ± 0.8	5.2 ± 0.4	1.0 ± 0.1
SW ND8	50.2 ± 0.3	1173 ± 68	50.8 ± 4.1	7.6 ± 0.3	1.0 ± 0.1
SW ND10	45.3 ± 0.6	966 ± 17	30.9 ± 4.9	4.6 ± 0.7	0.6 ± 0.2
SW 1D6	46.2 ± 0.1	1067 ± 30	42.9 ± 2.4	7.4 ± 0.9	0.8 ± 0.1
SW 1D8	51.1 ± 0.8	1056 ± 27	37.3 ± 3.4	4.7 ± 0.3	0.9 ± 0.2
SW 1D10	54.4 ± 1.3	1138 ± 28	36.0 ± 3.3	7.3 ± 0.9	0.6 ± 0.1
HW 1D6	53.8 ± 0.1	1062 ± 34	50.2 ± 6.8	4.3 ± 0.2	1.7 ± 0.3
HW 1D8	50.4 ± 0.9	1092 ± 28	42.0 ± 3.6	6.4 ± 0.7	0.9 ± 0.2
HW 1D10	46.2 ± 1.2	992 ± 55	46.6 ± 2.6	5.8 ± 0.4	1.1 ± 0.1

Abbreviations: Once-dried hardwood (HW 1D), Once-dried softwood (SW 1D), Never-dried softwood (SW ND)

excluded while calculating fitting parameters for the power law equation.

Since the HefCel grades were not completely fibrillated, the viscosity of the suspensions at low consistencies was quite low, and it was observed that those suspensions did not form gels below 5% consistency. Hence, the oscillatory studies were made for samples only at 7 and 10% solids. Amplitude (strain) sweep curves for all HefCel grades are not shown but can be accessed from the supplementary information along with respective frequency sweep curves. Selected results from the amplitude (strain) sweeps can be found in Fig. 6. The linear viscoelastic region (LVE) varied between samples but was typically found to be below 1% strain. Moreover, many samples exhibited no flow point until 100% strain. Both the storage and loss moduli increased with an increase in suspension consistency. It was observed that for the SW ND pulp, 6 mg/g enzyme dosage was sufficient to produce a stable gel above 7% solids but as the dosage was increased to 10 mg/g, the gel strength reduced with crossover occurring at roughly 2% strain for 10% SW 1D 10 sample. On the other hand, for hardwood-derived grades, an increase in enzyme dosage was found to enhance the gelling tendency of the suspensions.

Yield stress (τ_y) of the HefCel grades is shown in Fig. 6e at 7 and 10% consistencies. Data regarding yield stress of fibrillar CNMs at such high consistencies is rare in literature; however, numerous studies have reported τ_y values in the 0–1-3% consistency range. Nazari et al. reported τ_y values in the order of 1000 Pa at 7% consistency for CNF suspensions when quantified using several different methods (Nazari et al. 2016). In another work, Mohtaschemi et al. reported τ_y value of 33.9 Pa for a CNF suspension at 2.3% consistency, when measured using a vane geometry (Mohtaschemi et al. 2014). Therefore, in comparison of CNMs produced via mechanical grinding (or homogenization), HefCel grades possess much lower yield stress. Yield stress is an important rheological parameter for CNM suspensions when dealing with their mixing and pumping and lower τ_y values make HefCel a promising material for applications in coating and 3D printing.

Film properties

Finally, the performance of the HefCel grades was tested in a typical application for fibrillated celluloses, i.e. as standalone films. Extensive analysis of the prepared films was not undertaken as film formation was only used to demonstrate the self-assembling nature of HefCel grades. Therefore, any barrier tests were not in the scope of the current work. The films were found to be formed homogeneously but exhibited poor mechanical properties (* MERGEFORMAT Table 2). Both the tensile strength and strain at break of the films were much lower when compared to CNF films, where values greater than 100 MPa and 5%, respectively, have been reported (Syverud and Stenius 2009). However, such behavior was expected as the fibril dimensions are vastly different and a similar result has previously been reported by Rol et al. (2017). Comparison within HefCel grades shows that films made from SW ND10, SW 1D8 and SW 1D10

had lower tensile strength than other films while elongation at break remained similar. The overall low tensile strength of the HefCel films could pose challenges towards their industrial applicability. However, the film strength and elastic properties could be improved by using strength or plasticizing additives such as carboxymethylcellulose (CMC), hydroxyethylcellulose (HEC), sorbitol, etc. (Herrera et al. 2017; Hubbe et al. 2017a, b; Spoljaric et al. 2015).

Conclusions

Understanding the role of process parameters and raw materials could pave ways to produce cellulose nanomaterials with properties tuned for optimal performance in specific applications. The present work investigated the effect of enzyme dosage on the structure–property relationship in fibrillated cellulose materials produced via enzymatic treatment of wood pulp. The enzymatic treatment was done using the HefCel process developed at VTT, which produced fibrillated cellulose at 20% consistency. The effect of enzyme dosage level in the HefCel process was studied using three different types of pulp fibres as substrates, namely, never-dried softwood, once-dried softwood, and once-dried hardwood.

The results show that the enzyme hydrolysis action was not a direct function of enzyme dosage but rather dependent on the raw material composition. An increase in enzyme dosage did not universally correlate with the change in aspect ratio of the fibres and neither did it lead to a decrease in the average cellulose molar mass. Fibres in the softwood-derived HefCel grades showed a lower aspect ratio than the hardwood-derived grades. The different enzymatic action for softwood and hardwood substrates is hypothesized to be due to the presence of high amount of hemicelluloses in the hardwood pulp.

Both viscosity and water retention values of the HefCel suspensions were found to decrease with increasing enzyme dosage. The shear viscosity data was fitted with the power law equation $\tau = K.\dot{\gamma}^n$ where the power law index n was found to vary from 0.11 to 0.73. The shear-thinning behavior decreased with increasing consistency. The suspension viscosity was found to be highly dependent on the consistency as $\mu \sim c^m$, with m ranging from 2.75 to 4.31. Yield stress (τ_y) of the HefCel suspensions was measured at 7 and 10% consistencies and was found to be much lower than typical CNF grades. Future work on the topic could focus on studying different enzyme cocktails and investigate the performance of the HefCel grades in end-use applications such as 3D printing, coatings, and rheology modification. Moreover, future work could focus of studying the thixotropic nature of HefCel materials as thixotropy plays an important role in printing stability and object resolution during 3D printing and coating consolidation during coating processes. The behavior of various HefCel grades during subsequent mechanical processing, such as homogenization and fluidization, could also be explored where the mechanical processing would allow the production of CNMs with narrow size distribution from HefCel grades.

Acknowledgments The authors would like to acknowledge Janika Hart for assisting in microscopy and rheological characterization and Ulla Salonen for optical fibre analysis. We would also like to thank Atte Mikkelson for performing the SEC measurements.

Funding Open Access funding provided by Technical Research Centre of Finland (VTT). This work was part of the Academy of Finland Flagship Programme under project numbers 318890 and 318891 (Competence Center for Materials Bioeconomy, FinnCERES).

Compliance with ethical standards

Conflict of interest The authors declare that they have no conflict of interest.

References

Abdul Khalil HPS et al (2014) Production and modification of nanofibrillated cellulose using various mechanical processes: a review. Carbohyd Polym 99:649–665

Abitbol T et al (2016) Nanocellulose, a tiny fiber with huge applications. Curr Opin Biotechnol 39:76–88. https://www.sciencedirect.com/science/article/pii/S0958166916000045.

Ander P, Hildén L, Daniel G (2008) Cleavage of softwood kraft pulp fibres by HCl and cellulases. BioResources 3(2):477–490. https://ojs.cnr.ncsu.edu/index.php/BioRes/article/view/BioRes_03_2_0477_Ander_HD_Cleavage_Kraft_Fibers.

Baati R, Magnin A, Boufi S (2017) High solid content production of nanofibrillar cellulose via continuous extrusion. ACS Sustain Chem Eng 5(3):2350–2359

Berggren R, Berthold F, Sjöholm E, Lindström M (2003) Improved methods for evaluating the molar mass distributions of cellulose in kraft pulp. J Appl Polymer Sci 88(5): 1170–1179. https://doi.org/10.1002/app.11767 (February 17, 2020).

de Campos A et al (2013) Obtaining nanofibers from Curauá and Sugarcane Bagasse Fibers using enzymatic hydrolysis followed by sonication. Cellulose 20(3):1491–1500

Dimic-Misic K et al (2013) The role of MFC/NFC swelling in the rheological behavior and dewatering of high consistency furnishes. Cellulose 20(6):2847–2861. https://doi.org/10.1007/s10570-013-0076-3

Dufresne A (2019) Nanocellulose processing properties and potential applications. Curr Forest Reports 5(2):76–89. https://doi.org/10.1007/s40725-019-00088-1

Fang Z, Hou G, Chen C, Hu L (2019) Nanocellulose-based films and their emerging applications. Curr Opin Solid State Mater Sci 23(4):100764

Fernandes Diniz JMB, Gil MH, Castro JAAM (2004) Hornification—its origin and interpretation in wood pulps. Wood Sci Technol 37(6):489–494. https://doi.org/10.1007/s00226-003-0216-2 (August 14, 2019).

Gao W et al (2015) Effect of depth beating on the fiber properties and enzymatic saccharification efficiency of softwood kraft pulp. Carbohyd Polym 127:400–406

Gourlay K et al (2015) The use of carbohydrate binding modules (CBMs) to monitor changes in fragmentation and cellulose fiber surface morphology during cellulase- and swollenin-induced deconstruction of lignocellulosic substrates. J Biol Chem 290(5):2938–2945

Gourlay K, van der Zwan T, Shourav M, Saddler J (2018) The potential of endoglucanases to rapidly and specifically enhance the rheological properties of micro/nanofibrillated cellulose. Cellulose 25(2):977–986

Henriksson M, Henriksson G, Berglund LA, Lindström T (2007) An environmentally friendly method for enzyme-assisted preparation of microfibrillated cellulose (MFC) nanofibers. Euro Polymer J 43(8):3434–3441

Herrera MA., Mathew AP, Oksman K (2017) Barrier and mechanical properties of plasticized and cross-linked nanocellulose coatings for paper packaging applications. Cellulose 24(9):3969–3980. https://doi.org/10.1007/s10570-017-1405-8 (November 17, 2020).

Hidayat BJ, Felby C, Johansen KS, Thygesen LG (2012) Cellulose is not just cellulose: a review of dislocations as reactive sites in the enzymatic hydrolysis of cellulose microfibrils. Cellulose 19(5):1481–1493

Hidayat BJ et al (2015) The binding of cellulase variants to dislocations: a semi-quantitative analysis based on CLSM (Confocal Laser Scanning Microscopy) images. AMB Express 5(1):1–14

Hiltunen J, Kemppainen K, Pere J (2015) Process for producing fibrillated cellulose material.

Ho TTT, Abe K, Zimmermann T, Yano H (2015) Nanofibrillation of pulp fibers by twin-screw extrusion. Cellulose 22(1):421–433

Hoeger IC et al (2013) Mechanical deconstruction of lignocellulose cell walls and their enzymatic saccharification. Cellulose 20(2):807–818

Hu, J, V Arantes, A Pribowo, and J N. Saddler. 2013. "The synergistic action of accessory enzymes enhances the hydrolytic potential of a 'Cellulase Mixture' but is highly substrate specific." *Biotechnol Biofuels* 6(1): 112. http://biotechnologyforbiofuels.biomedcentral.com/articles/https://doi.org/10.1186/1754-6834-6-112 (February 27, 2020).

Hu J, Tian D, Renneckar S, Saddler JN (2018) Enzyme mediated nanofibrillation of cellulose by the synergistic actions of an endoglucanase, lytic polysaccharide monooxygenase (LPMO) and Xylanase. Sci Reports 8(1):1–8

Hubbe MA, Ferrer A et al (2017) Nanocellulose in thin films, coatings, and plies for packaging applications: a review. BioResources 12(1). http://ojs.cnr.ncsu.edu/index.php/BioRes/article/view/BioRes_12_1_2143_Hubbe_Review_Nanocellulose_Thin_Films_Coatings_Plies.

Hubbe MA, Tayeb P et al (2017) Rheology of nanocellulose-rich aqueous suspensions: a review. BioResources 12(4):9556–9661

Igarashi K et al (2011) Traffic jams reduce hydrolytic efficiency of cellulase on cellulose surface. Science 333(6047):1279–1282

Karim, Z, S Afrin, Q Husain, and Rc Danish. 2017. "Necessity of enzymatic hydrolysis for production and functionalization of nanocelluloses." *Crit Rev Biotechnol* 37(3): 355–70. https://www.tandfonline.com/doi/full/https://doi.org/10.3109/07388551.2016.1163322 (February 27, 2020).

Karppinen, A et al. 2012. "Flocculation of microfibrillated cellulose in shear flow." *Cellulose* 19(6): 1807–19. http://link.springer.com/https://doi.org/10.1007/s10570-012-9766-5.

Klar V et al (2019) Shape fidelity and structure of 3D printed high consistency nanocellulose. Sci Reports 9(1):1–10

Koponen AI (2019) The effect of consistency on the shear rheology of aqueous suspensions of cellulose micro- and nanofibrils: a review. Cellulose 27(4):1879–1897

Kumar V et al (2016) Roll-to-roll processed cellulose nanofiber coatings. Ind Eng Chem Res 55(12):3603–3613. https://doi.org/10.1021/acs.iecr.6b00417

Laureano-Perez L, Teymouri F, Alizadeh H, Dale BE (2005) Understanding factors that limit enzymatic hydrolysis of biomass: characterization of pretreated corn stover. In: Applied biochemistry and biotechnology—Part A enzyme

engineering and biotechnology. Springer, Heidelberg, pp 1081–1099.
Lehmonen J, Pere J, Hytönen E, Kangas H (2017) Effect of Cellulose Microfibril (CMF) addition on strength properties of middle ply of board. Cellulose 24(2):1041–1055
Liu H et al (2009) Visualization of enzymatic hydrolysis of cellulose using AFM phase imaging. Enzyme Microbial Technol 45(4):274–281
Malucelli LC et al (2019) Influence of cellulose chemical pretreatment on energy consumption and viscosity of produced cellulose nanofibers (CNF) and mechanical properties of nanopaper. Cellulose 26(3):1667–1681
Mohtaschemi M et al (2014) Rheological characterization of fibrillated cellulose suspensions via Bucket Vane Viscometer. Cellulose 21(3):1305–1312
Mosier N et al (2005) Features of promising technologies for pretreatment of lignocellulosic biomass. Biores Technol 96(6):673–686
Naderi A, Lindström T (2016) A comparative study of the rheological properties of three different nanofibrillated cellulose systems. Nord Pulp Pap Res J 31(3):354–363
Nazari B, Kumar V, Bousfield DW, Toivakka M (2016) Rheology of cellulose nanofibers suspensions: boundary driven flow. J Rheol 60(6):1151–1159. https://doi.org/10.1122/1.4960336 (September 16, 2020).
Pääkkö M et al (2007) Enzymatic hydrolysis combined with mechanical shearing and high-pressure homogenization for nanoscale cellulose fibrils and strong gels. Biomacromol 8(6):1934–1941. https://doi.org/10.1021/bm061215p
Penttilä PA et al (2013) Xylan as limiting factor in enzymatic hydrolysis of nanocellulose. Bioresource Technol 129:135–141
Pere J, Tammelin T, Niemi P, Lille M, Virtanen T, Penttilä PA, Ahvenainen P, Grönqvist S. (2020) Production of high solid nanocellulose by enzyme-aided fibrillation coupled with mild mechanical treatment. ACS Sust Chemi Eng. https://doi.org/10.1021/acssuschemeng.0c05202
Pettersen RC (1991) Wood sugar analysis by anion chromatography. J Wood Chem Technol 11(4):495–501
Plackett (2014) A review of nanocellulose as a novel vehicle for drug delivery. Nordic Pulp Paper Res J 29(01):105–118. http://www.npprj.se/html/xml/toc8908.html.
Quinlan RJ, Teter S, Xu F (2010) Development of cellulases to improve enzymatic hydrolysis of lignocellulosic biomass. Biochemical Conversion of Lignocellulosic Biomass, Elsevier Inc., In Bioalcohol Production, pp 178–201
Rahikainen J et al (2020) High consistency mechano-enzymatic pretreatment for kraft fibres: effect of treatment consistency on fibre properties. Cellulose.
Rol F et al (2017) Pilot-scale twin screw extrusion and chemical pretreatment as an energy-efficient method for the production of nanofibrillated cellulose at high solid content. ACS Sustain Chem Eng 5(8):6524–6531
Saarinen T et al (2014) The effect of wall depletion on the rheology of microfibrillated cellulose water suspensions by optical coherence tomography. Cellulose 21(3):1261–1275. https://doi.org/10.1007/s10570-014-0187-5 (November 17, 2020).
Sandås SE, Salminen PJ, Eklund DE (1989) Measuring the water retention of coating colors. Tappi J 72(12):207–210
Schenker M, Schoelkopf J, Gane P, Mangin P (2018) Influence of shear rheometer measurement systems on the rheological properties of microfibrillated cellulose (MFC) suspensions. Cellulose 25(2):961–976
Schenker M, Schoelkopf J, Gane P, Mangin P (2019) Rheology of Microfibrillated Cellulose (MFC) suspensions: influence of the degree of fibrillation and residual fibre content on flow and viscoelastic properties. Cellulose 26(2):845–860
Siqueira G et al (2010) Morphological investigation of nanoparticles obtained from combined mechanical shearing, and enzymatic and acid hydrolysis of sisal fibers. Cellulose 17(6):1147–1158
Siqueira G et al (2011) Mechanical properties of natural rubber nanocomposites reinforced with cellulosic nanoparticles obtained from combined mechanical shearing, and enzymatic and acid hydrolysis of sisal fibers. Cellulose 18(1):57–65
Siró I, Plackett D (2010) Microfibrillated cellulose and new nanocomposite materials: a review. Cellulose 17(3):459–494. https://doi.org/10.1007/s10570-010-9405-y.
Sluiter A et al (2012) NREL/TP-510–42618 Analytical procedure - determination of structural carbohydrates and lignin in biomass. Laboratory Analytical Procedure (LAP) 2011(April 2008):17. www.nrel.gov (February 17, 2020).
Song Q, Winter WT, Bujanovic BM, Amidon TE (2014) Nanofibrillated cellulose (NFC): a high-value co-product that improves the economics of cellulosic ethanol production. Energies 7(2):607–718. http://www.mdpi.com/1996-1073/7/2/607 (February 26, 2020).
Spoljaric S, Salminen A, Luong ND, Seppälä J (2015) Ductile nanocellulose-based films with high stretchability and tear resistance. Euro Polymer J69:328–340
Sumner JB, Noback V (1924) The estimation of sugar in diabetic urine, using dinitrosalicyclic acid. J Biol Chem 62(2):287–290. http://www.jbc.org/ (May 12, 2020).
Syverud K, Stenius P (2009) Strength and barrier properties of MFC films. Cellulose 16(1):75–85. https://doi.org/10.1007/s10570-008-9244-2.
Thygesen LG, Hidayat BJ, Johansen KS, Felby C (2011) Role of supramolecular cellulose structures in enzymatic hydrolysis of plant cell walls. J Ind Microbiol Biotechnol 38(8):975–983
Turpeinen T et al (2020) Pipe rheology of microfibrillated cellulose suspensions. Cellulose 27(1):141–156
Zhang J, Tang M, Viikari L (2012) Xylans inhibit enzymatic hydrolysis of lignocellulosic materials by cellulases. Bioresource Technol 121:8–12